

REDETERMINATION OF THE LEPIDOLITE- $2M_1$ STRUCTURE

TERESA H. SWANSON AND S. W. BAILEY

Department of Geology & Geophysics, University of Wisconsin-Madison
Madison, Wisconsin 53706

Abstract—The structure of a lepidolite- $2M_1$ from Biskupice, Czechoslovakia, has been redetermined. Violations of systematic extinctions and of monoclinic equivalences plus the results of a second harmonic generation test indicate that the true symmetry most likely is $C\bar{1}$. The deviation of the data set from $C2/c$ symmetry, however, proved to be too small to permit a statistically significant refinement in $C\bar{1}$. Refinement in $C2/c$ symmetry indicated no ordering of tetrahedral cations but ordering of octahedral cations so that $M(1) = Li_{0.93}R^{2+}_{0.06}Fe^{3+}_{0.01}$ and $M(2) = Al_{0.58}Li_{0.35}\square_{0.07}$. The tetrahedra are elongated to form trigonal pyramids with a rotation angle of 6.2° . The anomalous orientation of the thermal ellipsoid for the F,OH anion plus the large equivalent isotropic B value of 2.58 for F,OH and of 1.74 for the interlayer K cation, whose position is partly restricted in $C2/c$ symmetry, suggest a lower symmetry than $C2/c$.

The compositions of this sample and of a second lepidolite- $2M_1$ from Western Australia fall outside the stability field of lepidolite- $2M_1$ in the synthetic system. Structural control of the stacking sequence is discounted on the basis of the structural similarity of the lepidolite unit layers. Crystallization parameters are considered more important than composition or the structure of the unit layer in determining the stability and occurrence of different layer-stacking sequences in lepidolite.

Key Words—Crystal structure, Lepidolite, Lithium, Mica.

INTRODUCTION

Lepidolite crystallizes in nature primarily as the $1M$, $2M_2$, and $3T$ structural forms. Munoz (1968) was only able to synthesize the $1M$ and $2M_1$ structures hydrothermally in the lepidolite-muscovite system. Although both $1M$ and $2M_1$ forms crystallized together at many compositions, Munoz concluded that the $2M_1$ structure was the more stable form for trilithionite $[K(Li_{1.5}Al_{1.5})(Si_3Al)O_{10}(F,OH)_2]$ and probably also for all micas on the join from trilithionite to muscovite $[KAl_2(Si_3Al)O_{10}(OH,F)_2]$, for 25% of the range from trilithionite to polyolithionite $[K(Li_2Al)Si_4O_{10}F_2]$, and for 40% of the range from muscovite to polyolithionite (Figure 1). Munoz considered the apparent absence of lepidolite- $2M_1$ in nature as due to absence of the appropriate bulk compositions near trilithionite.

Trioctahedral lepidolite- $2M_1$ can be distinguished from dioctahedral Li-bearing muscovite- $2M_1$ by its Li content, cell dimensions, and X-ray diffraction intensities (especially of type $0k\ell$). To the best of our knowledge, the only reported occurrence of lepidolite- $2M_1$ in nature is in a Li-rich pegmatite near Biskupice, Czechoslovakia (Černý *et al.*, 1970). The structural refinement of a specimen from this locality was reported by Sartori (1977).

At the time of the Sartori publication we already had obtained a specimen of the Biskupice lepidolite from Dr. P. Černý with the intention of refining the structure. We decided to continue with our investigation for two reasons. First, analysis of the Sartori paper indicated, by comparison with our own data, that the diffraction data had been collected using the normal beta angle for a $2M_1$ structure of approximately 95° . But the beta angle

is listed in the paper as $99^\circ 7.5'$, as determined by Černý *et al.* (1970) from a powder pattern, and we have verified that the bond lengths and angles reported in the paper were calculated using the latter value. The latter value is close to the normal value for a $1M$ structure and can be used to define an acceptable alternate cell for the $2M_1$ structure as well. Usage of one cell to collect the data and a different cell to calculate the bond lengths, however, leads to an obvious bias in the results. Recalculation of the bond lengths with our own values of the cell dimensions showed differences from the published values ranging from 0.003 Å to 0.098 Å, with the magnitude of the error dependent on the direction of the individual bond. The average errors were 0.027 Å for individual T–O bonds, 0.032 Å for M–O bonds, and 0.062 Å for K–O bonds. Second, the Sartori refinement was based on 590 reflections recorded by the Weissenberg film method and could be refined only to an R_1 value of 11.3%. The structure of this interesting specimen is important enough to warrant a more detailed structural refinement for comparison with other lepidolite structures.

EXPERIMENTAL

The Biskupice lepidolite- $2M_1$ crystals proved to be of marginal quality for an accurate structure determination. Precession and Weissenberg photographs were taken of 35 crystal flakes, and the crystal showing the best spot shapes was selected for data collection. This crystal measured $0.3 \times 0.2 \times 0.03$ mm. Cell dimensions of $a = 5.199(1)$ Å, $b = 9.026(2)$ Å, $c = 19.969(5)$ Å, and $\beta = 95.41(2)^\circ$ were obtained on the crystal by least-squares refinement of 15 low- to medium-angle

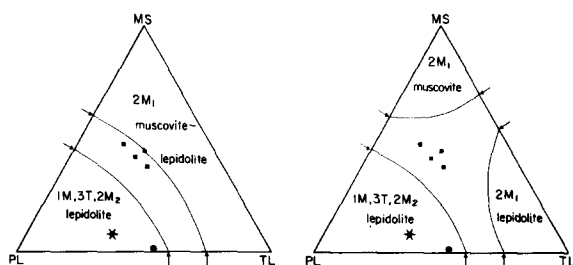


Figure 1. Two possible interpretations of discontinuities along joins in the synthesis study of Munoz (1968). Squares are natural two-phase micas, the asterisk is Biskupice- $2M_1$ of this study, and the circle is Londonderry lepidolite- $2M_1$.

reflections on an automated single crystal diffractometer. Černý *et al.* (1970) give refractive indices of $N_\alpha = 1.537$, $N_\beta = 1.552$, and $N_\gamma = 1.554$ for Biskupice lepidolite- $2M_1$. The optic axial plane is listed as normal to (010) with $2V = 22^\circ\text{--}28^\circ$. The measured and calculated densities are 2.828 g/cm³. Table 1 shows that an electron probe analysis of a flake cleaved from the same crystal as the platelet used for the structural refinement compares favorably with the wet chemical analysis of bulk material given by Černý *et al.* (1970) for this specimen. The latter composition has been used for this study and is shown on Figure 1 as an asterisk near the polyolithionite-trilithionite join.

Reflection intensities were measured in all eight octants of the limiting sphere to $2\theta = 60^\circ$ on a Nicolet P₂₁ automated single crystal diffractometer with graphite-monochromatized MoK α radiation. The data were collected in the $2\theta:\theta$ variable-scan mode. One standard reflection was checked after every 50 reflections to check electronic and crystal stability. A total of 5532 non-zero intensities was recorded. Reflections were considered observed if $I > 2\sigma(I)$. The integrated intensity I was calculated from $I = [S - (B_1 + B_2)]/B_r T_r$, where S is the scan count, B_1 and B_2 the backgrounds, B_r the ratio of background time to scan time, and T_r the 2θ scan rate in $^\circ/\text{min}$. $\sigma(I)$ was calculated from standard counting statistics. Integrated intensities were corrected for Lorentz and polarization factors and for absorption. The latter correction was empirical and based on comparison of the data to complete ψ scans (10° increments of ϕ) for selected reflections spaced at 2θ intervals of about 5° . The resulting structure amplitudes were averaged according to the requirements of both monoclinic and triclinic symmetry for refinement purposes.

REFINEMENT

For purposes of data collection the crystal was assumed to be C -centered, as indicated by the preliminary film data. The ideal space group for the $2M_1$ structure is $C2/c$. Analysis of the reflection indices and intensities, however, showed the presence of 12 $h0\ell$ reflec-

Table 1. Chemical analyses of Biskupice lepidolite- $2M_1$.

Oxide	Weight percentage		Cations per 11 O (anhydrous)		
	Wet ¹	Microprobe		Wet	Microprobe
SiO ₂	52.80	53.12	K	0.78	0.80
Al ₂ O ₃	19.94	20.17	Rb	0.06	0.06
Fe ₂ O ₃	0.38		Cs	0.02	0.02
FeO	0.055	0.03	Na	0.04	0.004
MnO	0.88	0.63	Ca	0.01	—
MgO	0.63	0.02			
TiO ₂	na ²	0.01	Li	1.61	1.65
CaO	0.11	nd ³	Fe ²⁺	0.005	0.002
Li ₂ O	5.91	6.00 ⁴	Mg	0.065	0.002
Na ₂ O	0.26	0.03	Mn	0.05	0.04
K ₂ O	9.00	9.15	Fe ³⁺	0.02	—
Rb ₂ O	1.36	1.36 ⁵	Ti	—	0.001
Cs ₂ O	0.75	0.75 ⁵	Al ^(VI)	1.17	1.24
H ₂ O	2.85	na			
F ₂	7.07	7.01	Al ^(IV)	0.42	0.38
			Si	3.58	3.62
	101.99	98.82			
—O = 2F	−2.98	−2.95			
Total	99.01	95.87 ⁶			

¹ Černý *et al.* (1970).

² Not analyzed.

³ Not detected.

⁴ Determined by atomic absorption.

⁵ Values taken wet chemical analysis.

⁶ Total does not include water.

tions (and 7 Friedel equivalents) that violated the systematic absences required by the c -glide plane (out of 175 $h0\ell$ observed), and 29 hkl and $hk\ell$ reflection pairs (and 22 Friedel equivalent pairs) that violated monoclinic intensity equivalences (out of 4292 total hkl observed). A second harmonic generation test of the sample by Bish *et al.* (1979) did not produce a signal, thus indicating centrosymmetry. These data indicate that the true space group is most likely $C\bar{1}$, but the deviation from $C2/c$ symmetry is very small. Refinements were conducted in space groups $C2/c$, $C2$, $C\bar{1}$, and $C1$.

Initial $C2/c$ refinement

Reflections violating monoclinic symmetry and the c -glide extinctions were deleted from the data set for this initial refinement, leaving a total of 971 observed and non-equivalent monoclinic reflections. The final atomic coordinates of Sartori (1977) were used as input, but with disordered octahedral cations. Scattering factors appropriate for 50% ionization were taken from Cromer and Mann (1968). Least-squares refinements with both sigma and unit weights were attempted; unit weights were found to give the most consistent results. The improvement with unit weights is believed due to the presence of two classes of reflections for layer silicates—strong $k = 3n$ reflections and weaker $k \neq 3n$ reflections. Because sigma is proportional to the square

Table 2. Atomic parameters for C2/c symmetry.

Atom	x	y	z	B _{equiv.} ¹	β ₁₁	β ₂₂	β ₃₃	β ₁₂	β ₁₃	β ₂₃
T (1)	0.4620 (4)	0.9230 (2)	0.1342 (1)	0.69	0.0027 (6)	0.0018 (2)	0.00075 (4)	-0.0009 (2)	0.0004 (1)	0.00005 (9)
T (2)	0.9572 (4)	0.7550 (2)	0.1342 (1)	0.78	0.0036 (6)	0.0016 (2)	0.00090 (5)	-0.0001 (2)	0.0003 (1)	0.00004 (9)
M (1)	0.25	0.75	0.0	1.89	0.0122 (46)	0.0045 (15)	0.0018 (4)	-0.0036 (20)	0.0014 (11)	-0.0011 (6)
M (2)	0.7569 (6)	0.5860 (4)	0.0000 (2)	0.66	0.0022 (10)	0.0017 (3)	0.00075 (7)	0.0001 (5)	0.0003 (2)	0.0002 (1)
K	0.0	0.0891 (3)	0.25	1.74	0.0122 (8)	0.0052 (3)	0.00138 (5)	0.0	0.0002 (2)	0.0
O (1)	0.4433 (11)	0.9262 (6)	0.0529 (3)	1.31	0.0074 (18)	0.0042 (6)	0.0011 (1)	-0.0029 (9)	0.0003 (4)	0.0002 (2)
O (2)	0.9173 (11)	0.7527 (6)	0.0529 (3)	1.31	0.0062 (19)	0.0051 (7)	0.0010 (1)	-0.0001 (8)	0.0002 (4)	0.0006 (2)
O (3)	0.9398 (12)	0.5882 (7)	0.1667 (3)	1.53	0.0146 (21)	0.0024 (6)	0.0014 (1)	0.0013 (9)	0.0009 (4)	-0.00001 (27)
O (4)	0.2358 (10)	0.8230 (6)	0.1631 (3)	1.24	0.0030 (16)	0.0045 (6)	0.0012 (2)	-0.0005 (8)	0.0001 (4)	0.0002 (2)
O (5)	0.7362 (12)	0.8542 (7)	0.1662 (3)	1.52	0.0102 (20)	0.0042 (6)	0.0013 (2)	0.0013 (9)	0.0004 (5)	-0.0001 (2)
F	0.4454 (14)	0.5720 (8)	0.0497 (3)	2.58	0.0347 (30)	0.0083 (8)	0.0008 (1)	0.0098 (13)	0.0002 (5)	0.0004 (3)

¹ Calculated from $B_{\text{equiv.}} = 4/3 [\beta_{11}/(a^*)^2 + \beta_{22}/(b^*)^2 + \beta_{33}/(c^*)^2]$.

root of the number of counts measured, the usual weighting scheme with $w = 1/\sigma^2$ unduly emphasizes the importance of one class of reflections relative to the other.

After several cycles of refinement of positional coordinates with program ORFLS, bond lengths indicated disorder of the tetrahedral cations but order of the octahedral cations with M(1) larger than M(2). The scattering factors for the octahedral cations were adjusted to fit the ordering pattern found by Sartori with $M(1) = \text{Li}_{0.92}\square_{0.08}$ and $M(2) = \text{Al}_{0.58}\text{Li}_{0.35}\text{Fe}^{3+}_{0.01}(\text{Mg}, \text{Mn}, \text{Fe}^{2+})_{0.06}$. Additional refinement varying positional coordinates and isotropic temperature factors and then anisotropic temperature factors reduced the residual R_1 to 9.5% for unit weights. The anisotropic factor for M(1) was non-positive definite at this stage. The structure would not refine further, and the hydrogen protons were not apparent on difference electron density maps.

C $\bar{1}$ refinement

The reflections violating monoclinic symmetry and the *c*-glide extinctions were added to the data set, and the former monoclinic equivalences were removed to create 1742 observed non-equivalent reflections for triclinic refinement. Subsequent least-squares cycles and electron density difference maps indicated slightly more electron density was needed in M(1) and less density in M(2). The ordering pattern was changed to $M(1) = \text{Li}_{0.93}(\text{Mg}, \text{Mn}, \text{Fe}^{2+})_{0.06}\text{Fe}^{3+}_{0.01}$ and $M(2) = \text{Al}_{0.58}\text{Li}_{0.35}\square_{0.07}$. Reflections that showed the greatest differences between F_0 and F_c were noted to have $F_0 > F_c$ consistently. Because the monitored check reflections indicated that the crystal had slipped twice during data collection, requiring new orientation matrix determinations by an automatic centering routine, the reflection data collected prior to each recentering were corrected at this time by a decay function to insure that all reflections were on the same scale factor.

With the new data set small semi-circular areas representing about 0.2 electrons above background were located on difference electron density maps at locations approximately those expected for the hydrogen protons associated with the OH groups. During subsequent cycles of least-squares refinement, the hydrogen positions (weighted according to the relative proportion of F and OH by analysis) were refined along with those of all other atoms, but the isotropic temperature factors of the hydrogens were held constant at 2.0. Refinement ceased at $R_1 = 9.5\%$ with all anisotropic temperature factors positive. No tetrahedral cation ordering was indicated. Because of the increased number of parameters, this refinement does not represent a statistically significant improvement over that in C2/c. As a result, further refinements were attempted in C1 and C2 symmetries.

C1 and *C2* refinements

In space group C1 the two M(2) octahedral sites are no longer related by symmetry and were designated M(2) and M(3). Two octahedral ordering patterns were postulated and their ideal atomic positions determined by the distance-least-squares program OPTDIS (W. A. Dollase, Department of Geology, University of California, Los Angeles, California 90024). In the first ordering pattern $M(2) = \text{Al}_{1.0}$ and $M(3) = \text{Al}_{0.16}\text{Li}_{0.70}\square_{0.14}$ and in the second pattern the contents of the two sites were reversed. The content of M(1) was held at its previous value. Each ordered model was refined through several least-squares cycles by varying only the M(2) and M(3) cations and their coordinating anions. Refinement ceased at 16.4% for model 1 and at 17.8% for model 2, indicating that C1 is not the correct space group.

The position of K(1) was held constant in order to fix the origin in this non-centrosymmetric space group, but the positions and temperature factors of all other atoms were varied. The residual R_1 decreased to 8.7% with

Table 3. Calculated bond lengths and angles.

<i>Bond lengths (Å)</i>		<i>Bond angles (°)</i>			
		Tetrahedron T(1)		around T(1)	
<i>to T(1)</i>					
O(1)	1.618(6)	O(1)–O(3)	2.703(9)	O(1)–O(3)	112.4(3)
O(3)	1.634(6)	O(4)	2.706(8)	O(4)	112.8(3)
O(4)	1.630(6)	O(5)	2.685(9)	O(5)	111.6(3)
O(5)	1.628(6)	O(3)–O(4)	2.616(9)	O(3)–O(4)	106.5(3)
mean	1.628	O(5)	2.615(9)	O(5)	106.5(3)
		O(4)–O(5)	2.611(9)	O(4)–O(5)	106.5(3)
		mean	2.656	mean	109.4
		Tetrahedron T(2)		around T(2)	
<i>to T(2)</i>					
O(2)	1.617(6)	O(2)–O(3)	2.708(8)	O(2)–O(3)	112.2(3)
O(3)	1.645(6)	O(4)	2.702(9)	O(4)	112.7(3)
O(4)	1.628(6)	O(5)	2.692(9)	O(5)	111.8(3)
O(5)	1.634(7)	O(3)–O(4)	2.624(9)	O(3)–O(4)	106.6(3)
mean	1.631	O(5)	2.624(9)	O(5)	106.3(3)
		O(4)–O(5)	2.619(9)	O(4)–O(5)	106.8(3)
		mean	2.662	mean	109.4
				<i>T1 to T2</i>	
				around O(3)	132.0(4)
				around O(4)	136.9(4)
				around O(5)	132.7(4)
				mean	133.9
		Octahedron M(1)			
<i>to M(1)</i>				<i>around M(1)</i>	
O(1) (× 2)	2.111(6)	O(1)–O(2) (× 2)	96.6(2)		
O(2) (× 2)	2.110(6)	F (× 2)	98.8(3)		
F (× 2)	2.100(6)	O(2)–F (× 2)	98.9(2)		
mean	2.107	mean (unshared)	98.1		
O(1)–O(2) (× 2)	3.151(8)	O(1)–O(2) (× 2)	83.4(2)		
F (× 2)	3.198(9)	F (× 2)	81.2(3)		
O(2)–F (× 2)	3.199(9)	O(2)–F (× 2)	81.1(2)		
	3.183	mean (shared)	81.9		
		Octahedron M(2)			
<i>to M(2)</i>				<i>around M(2)</i>	
O(1)	1.985(7)	O(1)–O(2)	96.2(3)		
	1.966(6)		95.8(3)		
O(2)	1.978(7)	O(1)–F	93.9(3)		
	1.969(7)		95.8(3)		
F	1.982(8)	O(2)–F	96.0(3)		
	1.981(8)		93.9(3)		
mean	1.977	mean (unshared)	95.3		
O(1)–O(2)	2.950(8)	O(1)–O(1)	82.8(3)		
	2.920(8)	O(2)	90.8(3)		
F	2.899(10)	F	87.4(3)		
	2.929(9)	O(2)–O(2)	82.7(3)		
O(2)–F	2.941(9)	F	87.7(3)		
	2.887(9)	F–F	77.6(3)		
mean (unshared)	2.921	mean (shared)	84.8		
O(1)–O(1)	2.613(9)				
O(2)	2.809(8)				
F	2.739(9)				
O(2)–O(2)	2.608(12)				
F	2.736(8)				
F–F	2.483(12)				
mean (shared)	2.665				

Table 3. Continued

to K	Interlayer cation	
	inner	outer
O(3) ($\times 2$)	2.951(6)	3.215(6)
O(4) ($\times 2$)	2.984(6)	3.269(6)
O(5) ($\times 2$)	2.957(7)	3.228(7)
mean	2.964	3.237

unit weights, but bond length calculations gave a number of unreasonable values. Thus, $C2/c$ is not considered to be the correct space group.

Final refinement as $C2/c$

Analysis of the atomic coordinates of the $C\bar{1}$ refinement showed that for all atoms the coordinates were within two standard deviations of the positions that would be generated by $C2/c$ symmetry and considerably less than one standard deviation for all but three parameters. The deviation of the data set from $C2/c$ symmetry is judged to be too small to permit refinement in a lower symmetry. Final refinement in $C2/c$ symmetry used the corrected monoclinic data set, input of the hydrogen proton, and the octahedral ordering pattern determined during refinement as $C\bar{1}$. The residual decreased from 9.5% to 9.1% with unit weights. Electron density difference maps were flat at all atomic positions at this stage. The fact that the residual did not decrease to the expected range of 4–5% is attributed to the quality of the crystal. Table 2 contains the resulting atomic coordinates and thermal parameters for the $C2/c$ refinement.¹ The hydrogen proton position at coordinates 0.58, 0.48, 0.07 is not included in Table 2 because of some doubt as to the reality of its determination (see next section).

DISCUSSION OF RESULTS

Table 3 gives calculated bond lengths and angles based on $C2/c$ symmetry. Figure 2 gives a polyhedral representation of the structure. The tetrahedral cations are disordered. The octahedral cations are ordered in the normal pattern for micas with M(1) larger than M(2) (Bailey, 1975). M–O, OH, F bond lengths calculated from the theoretical radii of Shannon (1976) are within 0.01 Å of the observed values for a composition of $M(1) = Li_{0.93}(Mg, Mn, Fe^{2+})_{0.06}Fe^{3+}_{0.01}$ and $M(2) = Al_{0.58}Li_{0.35}\square_{0.07}$ (with the vacancy included as Li and using $F_{0.76}OH_{0.24}$ per analysis). The composition derived from the structure is in good agreement with that derived by chemical analysis (Table 1). The ordering of Al into M(2) is consistent with the hypothesis of Guggenheim and Bailey (1977) that the small cation in

F-rich lepidolites and zinnwaldites should be ordered into the M(2) or M(3) sites, but no ordering between M(2) and M(3) could be proven in lower symmetry in this study. The individual bond lengths in Table 3 are different in most cases from those given by Sartori (1977), but in some cases the mean bond lengths are similar because of compensating \pm errors in the Sartori results. Many conclusions in the latter study, however, remain valid.

Table 4 lists other important structural features. The amount of tetrahedral rotation is small ($\alpha = 6.2^\circ$) because of the relatively good fit of the lateral dimensions of the tetrahedral and octahedral sheets. The tetrahedra are elongated to form trigonal pyramids with longer apical-to-basal oxygen bonds (mean = 2.698 Å) than basal-to-basal oxygen bonds (mean = 2.614 Å). As in other lepidolites, the tetrahedral cation is closer to the apical oxygen than to the basal oxygens so that the tetrahedral angles are unusually large ($\tau = 112.2^\circ$ and 112.3°).

The M(1) and M(2) octahedra are flattened and distorted. The values of $\psi = 60.7^\circ$ for M(1) and 58.6° for M(2) compared to the ideal value of 54.73° are measures of the flattening. The M(1) octahedron is severely distorted with $(\sigma_\theta)^2 = 72.8^\circ$ relative to M(2) with $(\sigma_\theta)^2 = 40.2^\circ$ (Table 4) and to the ideal value of 0° because of the need for the large M(1) octahedron to share edges with the smaller M(2) octahedra. The M(2) octahedron is distorted to a lesser degree and has alternate long and short edges depending on whether the adjacent octahedron is M(1) or M(2). The lengthening of edges shared with M(1) pulls anions away from their ideal positions and causes the bond lengths from M(2) to the upper O(1) and O(2) anions to be longer than those to the lower anions (Table 3, Figure 2).

The substitution of F for OH in the octahedral sheet causes another distortion of the structure. F is smaller than OH and allows a closer approach of the anion to the octahedral cation. The F–F shared edge is shortened and pulls the F, OH atoms away from their ideal positions directly under and over the K atoms in (001) projection (Figure 2).

The large equivalent isotropic B value of 2.58 for the ($F_{0.76}OH_{0.24}$) atom (Table 2) is a result of positional disorder of the two species involved plus a possible indication that the actual symmetry is lower than $C2/c$. Further evidence for the latter idea is the large $B = 1.89$

¹ A list of observed and calculated structure amplitudes can be obtained from the authors upon request.

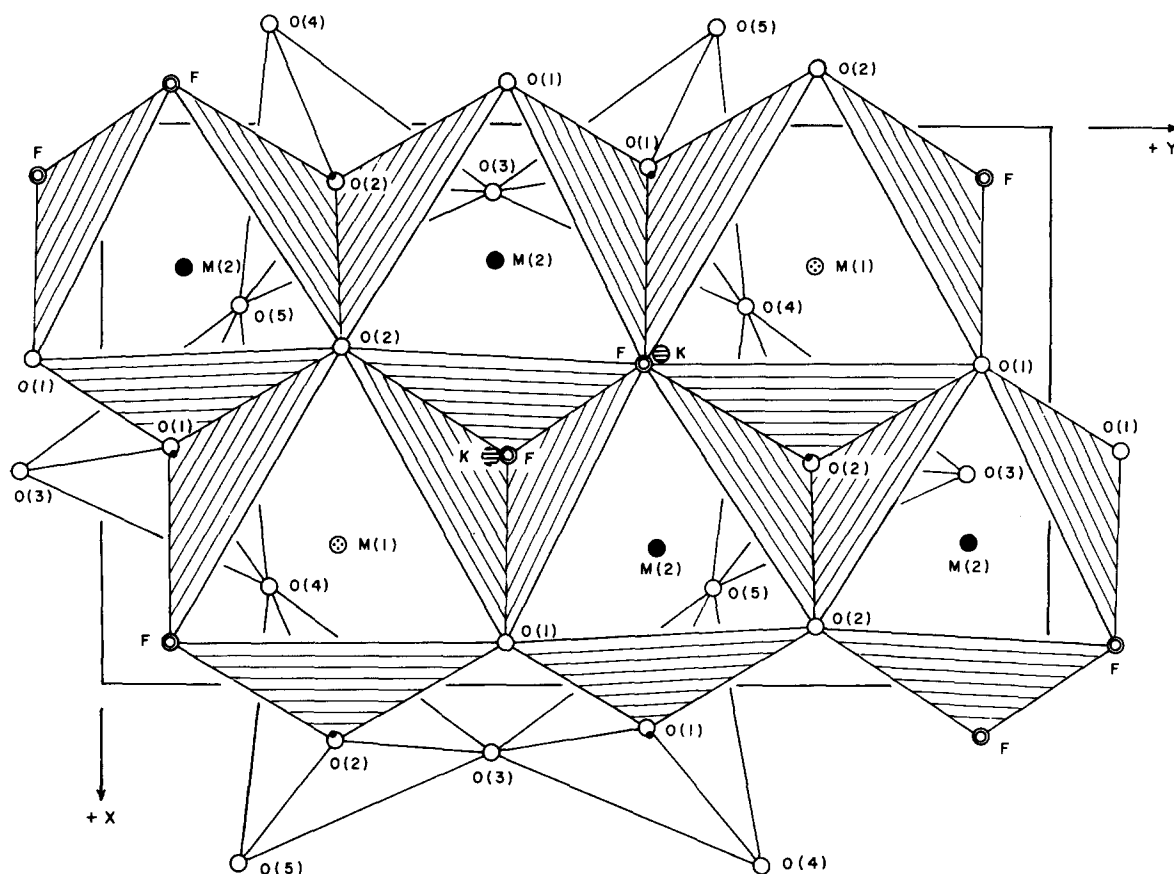


Figure 2. Polyhedral representation of the lepidolite structure. Only the lower tetrahedral sheet and the octahedral sheet of the first layer are shown.

value for M(1), whose position is fixed at $1/4, 3/4, 0$ in space group $C2/c$, whereas for M(2), whose position is not restricted by symmetry, $B = 0.66$ despite the larger substitution of atomic species in M(2). The similarly unrestricted tetrahedral cations have $B = 0.69$ and 0.78 despite more substitution than in M(1). The partly restricted K site at $0, y, 1/4$ also has a large B value of 1.74 .

The hydrogen bond angle ρ is defined by Giese (1979) as the angle between the O–H vector and (001) as measured with respect to the M(1) site. The composition of the M(1) and M(2) sites suggests that the hydrogen proton should point away from the octahedral sheet and away from M(2) toward the lower charge in M(1) with a predicted value from Giese's trioctahedral equation of 68.7° (Table 4). The observed angle is 151.5° with the hydrogen vector nearly parallel to (001) and pointing away from M(1). Although it is possible that this orientation is dictated in some manner by the layer stacking sequence, the large discrepancy more likely means that the hydrogen proton has not been located accurately, both because of its zero scattering power and its dilution by 76% F in that position. X-ray methods do not detect the hydrogen proton itself, only the hump of

excess electron density in the host oxygen caused by polarization by the proton. The O,F–H distance indicated by the determined positions is 1.2 \AA .

Table 5 lists the orientation of the anisotropic thermal ellipsoids for the structure. The major axes of the thermal ellipsoids for all atoms except F,OH are oriented approximately normal to the layers. The major axis of the ellipsoid for F,OH is halfway between X and Y in the XY plane. This cannot be due entirely to positional disorder of F and OH, because no similar effect is noted for the tetrahedral and octahedral cations. We suggest that this is additional evidence for a lower symmetry than $C2/c$ and possibly for a domain structure with a preference of Al to be associated with F (Kampf, 1977; Guggenheim and Bailey, 1977).

STABILITY OF THE $2M_1$ STRUCTURE IN LEPIDOLITE

Levinson (1953) noted a relationship between natural mica structures and their Li_2O contents. Micas with less than about 3.3% Li_2O were found to have the normal dioctahedral muscovite structure in his survey, those with 3.4–4.0% Li_2O were termed transitional and

Table 4. Structural features of lepidolite- $2M_1$.

Tetrahedral rotation α_{tet} (°)	6.2	
Tetrahedral angle τ_{tet} (°)	T (1):	112.3
	T (2):	112.2
Octahedral flattening ψ_{oct} (°)	M (1):	60.7
	M (2):	58.6
Octahedral distortion (°) ¹	RMS	$(\sigma\theta)^2$
	M (1):	5.7 72.8
	M (2):	4.3 40.2
Sheet thickness (Å)		
tetrahedral	2.256	
octahedral	2.061	
Interlayer separation (Å)	3.365	
Basal oxygen Δz (Å)	0.067	
Intralayer shift	0.358a ₃ , 0.358a ₂	
Layer offset	-0.003a ₁ , -0.003a ₁	
Resultant shift	-0.362a ₁	
β ideal (°)	94.98	

¹ RMS octahedral distortion parameter is defined by Dollase (1969) as the rms-deviation of the 15 octahedral angles from their ideal values. $\sigma\theta$ is defined by Robinson *et al.* (1971) as $(\sigma\theta)^2 = \sum_{i=1}^{15} (\theta_i - 90)^2/11$, where θ_i is the observed O-M-O angle.

contained a mixture of dioctahedral muscovite- $2M_1$ and a 6-layer trioctahedral lepidolite (now termed the $2M_2$ structure), those with 4.0–5.1% Li₂O generally had the $2M_2$ structure, and lepidolites with greater than 5.1% Li₂O had one of the structures now known as $1M$ and $3T$. Munoz (1968) advocated the separation of structures by plotting their compositions in the triangular diagram Ms–P1–T1 (Figure 1). This plot allows consideration of the tetrahedral Si,Al ratio and the number of octahedral vacancies, as well as octahedral Li content.

Levinson (1953) also noted several occurrences of a $2M_1$ "lithian muscovite" that he believed to be restricted to trioctahedral lepidolites with low Li₂O contents and to dioctahedral muscovites with relatively high Li₂O contents, although the upper and lower limits of Li₂O could not be given with certainty. These "lithian muscovites" were characterized by refractive indices in the lepidolite range and by $0k\ell$ intensities in which the 021 reflection was intensified and 020, 022, and 061 were decreased relative to the normal muscovite- $2M_1$ pattern (illustrated in Levinson's Figures 1 and 2). Lepidolite- $2M_1$ from Biskupice has these same characteristics, but in contrast to Levinson's samples, the Biskupice lepidolite has a high Li₂O content of 5.91%. In a survey of more than 50 lepidolite samples available in the University of Wisconsin collections, one additional sample was found that gave a similar $0k\ell$ diffraction pattern. This sample was a biaxial lepidolite from the Grosmont Mica Mine, Londonderry, Western Australia. Three analyses of this material gave Li₂O

Table 5. Anisotropic thermal ellipsoid orientations.

Atom	Axis	rms (Å) displacement	Angle to axes (°)		
			X	Y	Z
T(1)	r1	0.049 (8)	155 (6)	115 (6)	82 (3)
	r2	0.092 (5)	115 (6)	25 (6)	90 (7)
	r3	0.123 (4)	92 (4)	93 (7)	172 (3)
T(2)	r1	0.068 (6)	173 (18)	97 (18)	84 (3)
	r2	0.082 (5)	97 (18)	7 (17)	91 (4)
	r3	0.134 (4)	90 (3)	92 (4)	174 (3)
M(1)	r1	0.094 (29)	134 (25)	134 (21)	95 (17)
	r2	0.138 (23)	132 (25)	56 (23)	56 (15)
	r3	0.204 (21)	105 (13)	63 (18)	145 (14)
M(2)	r1	0.053 (13)	179 (16)	89 (16)	84 (6)
	r2	0.082 (8)	89 (17)	12 (9)	102 (9)
	r3	0.124 (6)	90 (5)	102 (9)	166 (8)
K	r1	0.129 (4)	172 (5)	90 (0)	92 (5)
	r2	0.147 (4)	90 (0)	0 (0)	90 (0)
	r3	0.167 (4)	82 (5)	90 (0)	178 (5)
O(1)	r1	0.076 (15)	148 (8)	121 (7)	83 (7)
	r2	0.142 (11)	65 (14)	131 (25)	54 (33)
	r3	0.155 (10)	72 (16)	123 (26)	143 (33)
O(2)	r1	0.092 (14)	177 (7)	93 (12)	87 (15)
	r2	0.124 (11)	90 (18)	131 (12)	41 (12)
	r3	0.160 (10)	87 (7)	139 (12)	131 (12)
O(3)	r1	0.095 (12)	73 (11)	163 (11)	94 (8)
	r2	0.140 (10)	157 (13)	107 (12)	70 (15)
	r3	0.169 (9)	105 (14)	92 (8)	159 (15)
O(4)	r1	0.064 (18)	174 (6)	95 (8)	89 (6)
	r2	0.134 (10)	93 (8)	19 (16)	108 (17)
	r3	0.161 (9)	84 (6)	108 (17)	162 (17)
O(5)	r1	0.110 (12)	30 (17)	120 (17)	94 (10)
	r2	0.139 (10)	60 (17)	31 (17)	87 (20)
	r3	0.162 (10)	86 (14)	85 (18)	175 (15)
F, OH	r1	0.117 (12)	113 (10)	55 (13)	133 (18)
	r2	0.141 (10)	117 (8)	56 (13)	43 (18)
	r3	0.257 (10)	143 (3)	127 (3)	88 (3)

contents of 5.06%, 5.56%, and 6.37%, so that it is definitely a second example of lepidolite- $2M_1$.

The Biskupice sample consists of small to medium size flakes of pink to purple color. Single crystal X-ray diffraction study showed both $2M_1$ and $1M$ polytypes to be present in a ratio of about 4:1. The Londonderry sample is quite different in appearance and consists of larger plates and books several centimeters in lateral extent that are colorless in thin flakes and maroon in thicker sections. The lepidolite crystals in the bulk of the pegmatite are uniaxial $3T$ polytypes, and the biaxial $2M_1$ crystals of similar composition are minor in abundance and segregated in occurrence (Simpson, 1927). The compositions of the Biskupice and Londonderry $2M_1$ lepidolites are plotted on Figure 1; both lie outside the stability field of $2M_1$ lepidolite in the synthetic system of Munoz (1968). Based on the present state of knowledge, composition does not seem to be the primary factor governing the formation of the $2M_1$ structure.

Several structural features of the Biskupice lepidolite

Table 6. Comparison of structural features for nine micas.

Structure	Cations Li	$\alpha(^{\circ})$	$\tau(^{\circ})$	Basal oxygen Δz (Å)	Sheet thickness (Å)			Oct. flattening $\psi(^{\circ})$		Oct. distortion ($^{\circ}$)		
					Tet.	Oct.	M(1)	M(2)	RMS			
					$\sigma(\theta)^2$			M(1)	M(2)	M(1)	M(2)	M(1)
Lepidolite- $2M_1$ (this study)	1.63	6.2	112.3	0.067	2.256	2.061	60.7	58.6	5.7	4.3	72.8	40.2
Lepidolite- $1M$ (Sartori, 1976)	1.69	7.4	112.2	0.063	2.255	2.060	60.8	58.5	6.0	5.6	74.6	41.2
Lepidolite- $2M_2$ (Sartori <i>et al.</i> , 1973)	1.69	6.5	111.9	0.086	2.241	2.074	60.8	58.4	6.7	4.6	74.1	39.5
Fluor-polythionite- $1M$ (Takeda and Burnham, 1969)	2.00	3.0	113.8	0.030	2.247	2.095	60.1	58.1	5.5	4.2	59.9	32.2
Lepidolite- $3T$ (Brown, 1978)	1.60	7.7	112.2	0.127	2.257	2.059	59.7	M (2) 60.9 M (3) 57.7	5.3	M (2) 5.4 M (3) 5.0	86.0	M (2) 88.3 M (3) 22.0
Biotite- $1M$ (Takeda and Ross, 1975)	—	7.6	110.4	0.014	2.271	2.138	59.2	58.9	4.9	4.7	40.6	37.2
Biotite- $2M_1$ (Takeda and Ross, 1975)	—	7.6	110.3	0.016	2.269	2.135	59.1	58.8	4.3	4.5	41.4	40.3
Zinnwaldite- $1M$ (Guggenheim and Bailey, 1977)	0.67	5.8	111.1	0.124	2.252	2.078	60.8	M (2) 56.5 M (3) 60.9	7.1	M (2) 3.0 M (3) 7.0	97.4	M (2) 8.0 M (3) 98.4
Muscovite- $2M_1$ (Güven, 1971)	—	11.4	111.0	0.223	2.339	2.103	—	57.0	9.8	4.8	106.2	57.3

lite- $2M_1$ have been compared with those of four other lepidolites, three other trioctahedral micas, and a dioctahedral muscovite to determine if these features influence the stacking sequences. The results are shown in Table 6. Although expected differences between the lepidolites, other trioctahedral micas, and muscovite exist, the Biskupice lepidolite- $2M_1$ specimen cannot be distinguished from the other lepidolites on the basis of Li content, tetrahedral twist angle, tetrahedral bond angle, basal corrugation, octahedral sheet thickness, octahedral flattening, or octahedral distortion.

Takeda and Ross (1975) analyzed the structures of coexisting $1M$ and $2M_1$ biotites and found a difference in the unit layers of the two structures. The apical oxygens and OH groups forming the upper and lower octahedral triads were found to be shifted as units along the $\pm Y$ directions so that the octahedral shared edges were rotated by about 6° . They suggested that these layer differences resulted from the atomic and geometric restraints imposed by adjacent layers arranged in different stacking sequences. Although the lepidolite- $1M$ in the Biskupice sample has not been analyzed structurally, comparison of the Biskupice lepidolite- $2M_1$ with the polyolithionite- $1M$ of Takeda and Burnham (1969) and with the lepidolite- $1M$ of Sartori (1976) shows no differences of the sort described above for biotite. This relationship can be seen qualitatively in Figure 2, where the octahedral shared edges are essentially parallel to the X-axis rather than being rotated. The unit layers of the $1M$ and $2M_1$ lepidolites are similar. The present data agree with those reported by Sartori (1976) who concluded, on the basis of comparison of the structural details of $1M$ and $2M_2$ lepidolites of the same composition, that the structure does not exert a strong control on the stacking sequence of layers.

Chaudhry and Howie (1973) in a study of lepidolites from the Meldon aplite concluded that a segregation of structural types could be found according to crystallization environment. They found $2M_2$ lepidolites in volatile-rich low-temperature pegmatites and pegmatitic veins cutting the aplite, whereas the $1M$ lepidolites were in the relatively volatile-poor and higher-temperature environment of the aplite itself. No information is available on the nature of the Biskupice pegmatite of the present study, but Simpson (1927) pointed out for the Grosmont pegmatite of Western Australia that the lepidolite in the bulk of the pegmatite is uniaxial. The biaxial lepidolite, identified in the present study as the $2M_1$ structural form, is restricted to the footwall in the immediate vicinity of thin veins of topaz, suggesting an analogy with the Meldon lepidolites cited above.

Baronnet (1975) studied the microtopography of micas, including F-polyolithionite, as synthesized under both dry and wet conditions. Micas in the dry system tended to grow almost entirely layer-by-layer, whereas

those grown in an excess of water developed abundant screw dislocations after initial layer-by-layer growth. Although these observations offer no specific clues as to the conditions that favor crystallization of the $2M_1$ structure, they do indicate a difference in the mechanism of crystal growth under different conditions. Thus, the evidence to date suggests that one or more of the parameters of crystallization (temperature, pressure, volatiles, degree of saturation, and rate of cooling) are more important than the composition or the structure of the unit layer in determining the stability and the occurrence of different layer stacking sequences in lepidolites.

ACKNOWLEDGMENTS

This research was supported in part by grant EAR78-05394 from the National Science Foundation and in part by grant 11224-AC2 from the Petroleum Research Fund, administered by the American Chemical Society. We acknowledge with thanks Dr. P. Černý for supplying the sample and C. A. Geiger for the electron microprobe analysis.

REFERENCES

- Bailey, S. W. (1975) Cation ordering and pseudosymmetry in layer silicates: *Amer. Mineral.* **60**, 175–187.
- Baronnet, A. (1975) L'aspect croissance du polymorphisme et du polytypisme dans les micas synthétiques d'intérêt pétrologique: *Fortshcr. Mineral.* **52**, 203–216.
- Bish, D. L., Horsey, R. S., and Newnham, R. E. (1979) Acentricity in the micas: an optical second harmonic study: *Amer. Mineral.* **64**, 1052–1055.
- Brown, B. E. (1978) The crystal structure of a $3T$ lepidolite: *Amer. Mineral.* **63**, 332–336.
- Černý, P., Rieder, M., and Povondra, P. (1970) Three polytypes of lepidolite from Czechoslovakia: *Lithos* **3**, 319–325.
- Chaudhry, M. N. and Howie, R. A. (1973) Lithium-aluminum micas from the Meldon aplite: *Mineral. Mag.* **39**, 289–296.
- Cromer, D. T. and Mann, J. B. (1968) X-ray scattering factors computed from numerical Hartree-Fock wave functions: *Acta Crystallogr.* **A24**, 321–324.
- Dollase, W. A. (1969) Crystal structure and cation ordering of piemontite: *Amer. Mineral.* **54**, 710–717.
- Giese, R. F., Jr. (1979) Hydroxyl orientations in 2:1 phyllosilicates: *Clays & Clay Minerals* **27**, 213–223.
- Guggenheim, S. and Bailey, S. W. (1977) The refinement of zinnwaldite- $1M$ in subgroup symmetry: *Amer. Mineral.* **62**, 1158–1167.
- Güven, N. (1971) The crystal structures of $2M_1$ phengite and $2M_1$ muscovite: *Z. Kristallogr.* **134**, 196–212.
- Kampf, A. R. (1977) Minyulite: its atomic arrangement: *Amer. Mineral.* **62**, 256–262.
- Levinson, A. A. (1953) Studies in the mica group: relationship between polymorphism and composition in the muscovite-lepidolite series: *Amer. Mineral.* **38**, 88–107.
- Munoz, J. L. (1968) Physical properties of synthetic lepidolites: *Amer. Mineral.* **53**, 1490–1512.
- Robinson, K., Gibbs, G. V., and Ribbe, P. H. (1971) Quadratic elongation: a quantitative measure of distortion in coordination polyhedra: *Science* **172**, 567–570.
- Sartori, F. (1977) The crystal structure of a $2M_1$ lepidolite: *Tschermak's Mineral. Petrogr. Mitt.* **23**, 65–75.

- Sartori, F. (1977) The crystal structure of a $2M_1$ lepidolite: *Tschermak's Mineral. Petrogr. Mitt.* **24**, 23–37.
- Sartori, F., Franzini, M., and Merlino, S. (1973) Crystal structure of a $2M_2$ lepidolite: *Acta Crystallogr.* **B29**, 573–578.
- Shannon, R. D. (1976) Revised effective ionic radii and systematic studies of interatomic distance in halides and chalcogenides: *Acta Crystallogr.* **A32**, 751–767.
- Simpson, E. S. (1927) Contributions to the mineralogy of Western Australia: *J. Royal Soc. W. Australia* **13**, 37–48.
- Takeda, H. and Burnham, C. W. (1969) Fluor-polyolithionite: a lithium mica with nearly hexagonal $(\text{Si}_2\text{O}_5)^{2-}$ ring: *Mineral. J.* **6**, 102–109.
- Takeda, H. and Ross, M. (1975) Mica polytypism: dissimilarities in the crystal structures of coexisting $1M$ and $2M_1$ biotite: *Amer. Mineral.* **60**, 1030–1040.

(Received 25 September 1980; accepted 29 November 1980)

Резюме—Структура Бискупичского (Чехословакия) лепидолита- $2M_1$ была повторно определена с большой точностью. Нарушения систематических экстинкции и моноклиных эквивалентности, а также результаты анализа по генерированию вторичной гармонике указывают, что истинная симметрия это, наиболее вероятно, $C\bar{1}$. Отклонение группы данных от $C2/c$ симметрии, однако, слишком мало, чтобы допустить статически значительное улучшение $C\bar{1}$. Улучшение в $C2/c$ симметрии указывает на неупорядоченность тетраэдрических катионов, а упорядоченность октаэдрических катионов, так что $M(1) = \text{Li}_{0,93}\text{R}^{2+}_{0,06}\text{Fe}^{3+}_{0,01}$ и $M(2) = \text{Al}_{0,58}\text{Li}_{0,35}\square_{0,07}$. Для образования тригональных пирамид с углом поворота $6,2^\circ$ тетраэдры являются вытянутыми. Аномальная ориентация термальной эллипсоиды для F,OH аниона, а также большая величина эквивалентного изотропного $B = 2,58$ для F,OH и $1,74$ для межслойного катиона K, положение которого в $C2/c$ симметрии частично ограничено, указывают на более низкую симметрию, чем $C2/c$.

Составы образцов чехословацкого и другого западно-австралийского лепидолита- $2M_1$ находятся вне поля устойчивости лепидолита- $2M_1$ в синтетической системе. Структурное регулирование последовательности укладки слоев игнорируется на основе структурного подобия элементарных слоев лепидолита. По сравнению с составом или структурой элементарного слоя, кристаллизационные параметры считаются более важными для определения устойчивости и наличия различных последовательностей укладки слоев в лепидолите. [E.C.]

Resümee—Die Struktur eines $2M_1$ -Lepidolit von Biskupice, Tschechoslowakei, wurde verfeinert. Die Verletzung der systematischen Auslöschungsregeln einerseits und der monoklinen Äquivalenzen andererseits sowie die Ergebnisse eines Testes auf Erzeugung der zweiten harmonischen Analyse weisen darauf hin, daß die wahre Symmetrie vom Typ $C\bar{1}$ ist. Die Abweichung der Daten von der $C2/c$ -Symmetrie erwies sich jedoch als zu klein, um eine signifikante statistische Verfeinerung in $C\bar{1}$ zu erlauben. Die Verfeinerung in der $C2/c$ -Symmetrie deutete auf keine Ordnung der Tetraederkationen hin, jedoch auf eine Ordnung der Oktaedern, so daß $M(1) = \text{Li}_{0,93}\text{R}^{2+}_{0,06}\text{Fe}^{3+}_{0,01}$ und $M(2) = \text{Al}_{0,58}\text{Li}_{0,35}\square_{0,07}$ ist. Die Tetraeder sind so gestreckt, daß trigonale Pyramiden mit einem Rotationswinkel von $6,2^\circ$ entstehen. Die anomale Orientierung des thermischen Ellipsoids für das F,OH-Anion und der große äquivalente isotrope B-Wert von $2,58$ für F,OH, sowie von $1,74$ für das Zwischenschicht-Kalium-Kation (dessen Lage zum Teil auf $C2/c$ -Symmetrie beschränkt ist) deuten auf eine niedrigere Symmetrie als $C2/c$ hin.

Die Zusammensetzung dieser Probe und eines weiteren $2M_1$ -Lepidolit von Westaustralien liegen im synthetischen System außerhalb des Stabilitätsfeldes von $2M_1$ -Lepidolit. Die strukturelle Beeinflussung der Stapelfolge ist abhängig von der strukturellen Ähnlichkeit der Lepidolitschichten. Die Kristallisationsbedingungen werden für die Stabilität und das Auftreten verschiedener Abfolgen der Einheitslage im Lepidolit für wichtiger gehalten als die Zusammensetzung oder die Struktur der Einheitschicht. [U.W.]

Résumé—La structure d'une lépidolite- $2M_1$ de Biskupice, Tchecoslovaquie, a été redéterminée. Des violations d'extinctions systématiques et d'équivalences monocliniques, plus les résultats d'un test de seconde génération harmonique indiquent que la symétrie réelle est vraisemblablement $C\bar{1}$. La déviation des données de la symétrie $C2/c$, cependant, a prouvé être trop petite pour permettre un raffinement statistiquement significatif dans $C\bar{1}$. Un raffinement dans la symétrie $C2/c$ n'a indiqué aucun rangement de cations tétraédres, mais un rangement de cations octaédres tels que $M(1) = \text{Li}_{0,93}\text{R}^{2+}_{0,06}\text{Fe}^{3+}_{0,01}$ et $M(2) = \text{Al}_{0,58}\text{Li}_{0,35}\square_{0,07}$. Les tétraédres sont allongés pour former des pyramides trigonales avec un angle de rotation de $6,2^\circ$. L'orientation anormale de l'ellipsoïde thermique de l'anion F,OH plus la large valeur équivalente isotropique de B de $2,58$ pour F,OH et de $1,74$ pour le cation intercouche K dont la position est partiellement restreinte dans la symétrie $C2/c$, suggère une symétrie plus basse que $C2/c$.

Les compositions de cet échantillon et d'une seconde lépidolite- $2M_1$ d'Australie de l'Ouest tombent en dehors du champ de stabilité de lépidolite- $2M_1$ dans le système synthétique. Le contrôle structural de la séquence d'empilement est rejeté à cause de la similarité structurale des couches unitaires de lépidolite. Les paramètres de cristallisation sont considérés être plus importants que la composition ou la structure de la couche unitaire dans la détermination de la stabilité et l'occurrence de différentes séquences d'empilement de couches dans la lépidolite. [D.J.]